npj | science of food

Article

Published in partnership with Beijing Technology and Business University & International Union of Food Science and Technology

https://doi.org/10.1038/s41538-025-00410-1

Dynamic membrane changes and osmotic effects by sugar alcohols

Lichun Chen[1,2], Feng Yao[1], Songwen Xue[1], Kuang Yao[1], Yun Huang[1], Huimin Zhao[1] & Qiong Shao[3] ✉

Sugar alcohols are natural sweeteners with various physiological functions, commonly used in low-calorie foods and pharmaceuticals. Current research primarily focuses on their sweetening properties and metabolic effects, often overlooking their interactions with cell membranes. This study built a giant phospholipid vesicle model to examine vesicle deformation in erythritol (Ery) and xylitol (Xyl) environments. The permeation of these sugar alcohols through real cell membranes was also investigated. Fluorescence microscopy and zeta potential measurements showed that osmotic stress from concentration gradients disrupted vesicle membrane structure. Ery and Xyl reduced ROS levels in HEK-293 cells and influenced membrane permeability. Notably, Xyl increased vesicle adsorption on the cell membrane at the same concentration. The findings indicate that sugar alcohols interact with membrane lipids through hydrogen bonds or other non-covalent interactions, modifying cell membrane structure and properties, thus providing a theoretical foundation for understanding their role in physiological environments.

In recent years, an increasing number of studies have shown that excessive consumption of refined sugars is associated with weight gain[1], obesity, diabetes, and metabolic syndrome[2–4]. For this reason, low-calorie or no-calorie sweeteners, such as sugar alcohols, have gained popularity as safer alternatives to daily sugar intake. Sugar alcohols are naturally occurring sweet compounds with different numbers of hydroxyl groups. Sugar alcohols are closely related to lipid metabolism in the human body. Animal experiments conducted by Kikuko et al. demonstrated that xylitol can influence metabolic parameters in rats and reduce the accumulation of visceral fat. This may be due to xylitol enhancing the expression of genes related to fatty acid oxidation in the liver, thereby promoting fat breakdown and the fatty acid oxidation process[5]. Kishore et al. also confirmed this perspective, suggesting that the intake of xylitol may help prevent the development of obesity and metabolic disorders[6]. However, not all studies support the positive effects of sugar alcohols on lipid metabolism. Some research has indicated that sugar alcohols do not improve dyslipidemia induced by a high-fat diet[7]. Under physiological conditions, when high doses of sugar alcohol are consumed, intestinal epithelial cells may be directly exposed to a high-concentration sugar alcohol environment[3]. Additionally, after absorption, the ingested sugar alcohols must pass through renal filtration[8]. With excessive intake, renal tubular cells may also be exposed to high concentrations of sugar alcohols during the processes of filtration and reabsorption. Therefore, in-depth research on the effects of sugar alcohols on cells is crucial for understanding their mechanisms of action in physiological environments. In addition, some studies have shown that these sugar alcohols can induce oxidative stress, exhibit anticancer activity[9–11], prevent dental caries[12] and affect bacterial virulence[13,14].

Despite the widespread use of sugar alcohols in food and medicine, modern research often overlooks their specific effects on cell membranes. Existing studies have shown that sugars influence the physical properties and functions of cell membranes through various mechanisms, including altering membrane fluidity and stability, participating in cell signaling, regulating intercellular recognition and adhesion, affecting membrane transport, and engaging in reactions related to oxidative stress and glycosylation[15]. However, the specific effects of sugar alcohols on cell membranes are still rarely reported, despite their potential influence being determined by the solute's chemical nature and the composition of the lipid bilayer. Therefore, further research on the biophysical effects of sugar alcohols at the cellular level is crucial for improving our understanding of their mechanisms, as well as their safety assessment and practical applications.

The cell membrane serves as the primary interface between the cell and its external environment. Consequently, it plays a crucial role in various cellular functions, including protection, selective permeability for substances, maintenance of cell potential, and cell signaling[16]. However, due to the complexity of membranes, studying the fundamental functional processes both in vivo and in vitro is challenging. So far, model cells have been extensively developed because they exhibit physicochemical properties

[1]Food Safety Key Laboratory of Zhejiang Province, School of Food Science and Biotechnology, Zhejiang Gongshang University, Hangzhou, China. [2]Physical Chemistry and Soft Matter, Wageningen University and Research, Wageningen, WE, Netherlands. [3]China National Bamboo Research Center, Key Laboratory of State Forestry and Grassland Administration on Bamboo Forest Ecology and Resource Utilization, Hangzhou, Zhejiang, PR China. ✉e-mail: planeplant@126.com

similar to natural cell membranes, particularly giant unilamellar vesicles (GUVs), which have become essential tools for examining the biophysical properties and dynamic behaviors of membranes. They provide a straightforward and controllable platform to simulate and investigate various functions and characteristics of cell membranes[17]. Tian et al. used the liposome vesicle model as an artificial cell model to study its interaction with microdroplets and simulated cell endocytosis, efflux, osmosis, and other behaviors[18]. Vesicle models have been employed to study the effects of different factors on membrane structure and function, including osmotic pressure, membrane composition, and interactions with external substances. As vesicles can closely mimic the bilayer structure and dynamic nature of cell membranes, their applications are increasingly expanding in fields such as drug delivery, membrane protein research, and cell signaling[19,20].

One of the crucial environmental factors is osmotic stress, which significantly impacts the stability of biological membranes. The passive osmotic mechanism of biological membranes holds substantial research value in the life sciences[21]. At present, many studies have demonstrated that differences in transmembrane permeability lead to phase separation of vesicles[22–25]. Due to the presence of protein mechanisms regulating osmosis in cell membranes, they can sensitively manage water within the membrane when there is an increase in osmotic pressure from the environment[23]. Currently, it has been shown that certain concentrations of glucose and sucrose can elicit vesicle budding behavior or produce membrane pores[25]. Some studies have found that increased osmotic pressure, such as salt stress and sugar stress, can cause phase separation and morphological changes in biofilms. Under high osmotic pressure, lipid vesicles may undergo deformation from vesicles to tubular structures, affecting their stability and function[26]. Additionally, changes in osmotic pressure have also been found to induce alterations in the mechanical properties of lipid bilayers in biofilms, such as changes in membrane rigidity and elasticity, which have important implications for understanding the physiological function of membranes[27]. However, the shape and structural changes of vesicles in the osmotic environment induced by sugar alcohol still require further investigation.

To gain a deeper understanding of the effects of sugar alcohols on cell membranes, this study constructed a giant phospholipid vesicle model to investigate the effects of Ery and Xyl on membrane permeability and structure under different concentration environments. Using fluorescence microscopy and zeta potential measurements, we examined the morphological changes of vesicle membranes and their impact on membrane permeability in the presence of sugar alcohol concentration gradients. Finally, using HEK-293 cells as a biological model, we further evaluated cell viability, intracellular ROS levels, membrane adsorption properties, and membrane potential changes in the presence of these sugar alcohols. This study aims to elucidate the comprehensive effects of sugar alcohols on cell membrane properties, providing a scientific basis for their safer and more effective application in industry and medicine.

Results and discussion

Significant alterations in vesicle morphology triggered by erythritol concentration

GUVs have an uninterrupted enclosed bilayer with a similar membrane structure to cells and can be used to simulate cell membranes in in vitro experiments. As shown in Supplementary Fig. 1a, POPC phospholipid molecules, which contain both hydrophilic and hydrophobic groups, can self-assemble into giant phospholipid vesicles under suitable conditions. The probe DiI binds to POPC phospholipid molecules, producing red fluorescence and uniformly labeling the vesicles, allowing the vesicle membrane boundaries to be clearly observed (Supplementary Fig. 1b). The particle size of the giant phospholipid vesicles was measured using a laser particle size analyzer. As shown in Supplementary Fig. 1c, the particle size of the giant phospholipid vesicles is primarily distributed in the range of 5–25 μm, making them suitable for experimental observation. Zeta potential is a measure of the strength of repulsion or attraction between particles and is closely related to the stability of the solution system. The higher the absolute value of the potential, the more stable the solution system. POPC is classified as a zwitterionic lipid, possessing both positive and negative charges, which can vary depending on the pH and ionic strength of the environment. In our study, we measured the zeta potential of the phospholipid vesicle solution under physiological conditions, which ranged from 0 to -20 mV (Supplementary Fig. 1d). This range is consistent with previous reports that consider the complex interplay of environmental factors such as pH and ion concentration, which can influence the net charge of POPC vesicles[28,29]. Therefore, our measurements reflect the behavior of POPC in a more physiologically relevant context, rather than in an idealized or isolated system.

An imbalance in osmotic pressure between the interior and exterior of the vesicle led to the outward diffusion of water molecules, resulting in an increase in internal pressure, thereby altering the shape of the glycerolipid vesicle (GLV) membrane. To systematically investigate the deformation behavior of vesicles under osmotic conditions induced by varying concentrations of sugar alcohols, we conducted a study examining the relationship between the deformation of pure POPC vesicles and the concentration of sugar alcohols. As illustrated in Supplementary Fig. 2, upon addition of sugar alcohols to the vesicle solution, a non-equilibrium state was initiated. Due to the unique chemical properties of sugar alcohols, they cannot freely diffuse through the cell membrane. With increasing sugar alcohol concentration, the concentration gradient of sugar alcohols between the interior and exterior of the vesicle membrane increased, resulting in a corresponding driving force for diffusion from the exterior to the interior of the membrane. Additionally, the increase in concentration induced an elevation in external osmotic pressure, driving water molecules to diffuse from the interior to the exterior of the vesicle membrane. Concurrently, the phospholipid vesicle membrane undergoes stretching to accommodate the osmotic stress, resulting in thinning of the phospholipid bilayer and consequent instability and morphological changes in the vesicle membrane structure. As depicted in Supplementary Fig. 3, the morphological changes of the vesicles within 60 s were tracked and recorded. At Ery concentrations of 1 mM and 5 mM, no significant morphological changes were observed compared to T_{0+} s, indicating that the same concentration did not induce substantial osmotic stress over time to cause visible deformation. However, at 10 mM, wrinkling of the vesicle membrane began to occur, and at 20 mM, significant morphological changes in the vesicles were observed, including budding and multicompartment formation. These results suggest that the morphological changes in GUVs are directly correlated with the concentration of Ery, with higher concentrations inducing more pronounced osmotic stress and subsequent membrane deformation. Under high osmotic pressure, the phospholipid vesicle membrane buds outward at 15 s, followed by a transition into vesicles with multiple compartments at 30 s; continuous changes in vesicle morphology occurred as the phospholipid membrane flowed.

Vesicles were positioned and analyzed by Image J software, as shown in Fig. 1a. The vesicle diameter was analyzed along the diagonal line, and then the data as shown in the figure on the right was obtained. At Ery concentrations of 1, 5 and 10 mM, there was no significant change in vesicle diameter at 0 s compared with 60 s. However, it was seen from the right figure that the vesicle diameter changed when the Ery concentration was at 20 mM. These results of this experiment were consistent with numerous prior studies, indicating that vesicle deformation or daughter vesicle formation was response to osmotic stress and osmotic gradient could induce fission[30,31]. In addition, the permeability of vesicle membranes to specific substances could be altered as a result of vesicle deformation. Furthermore, we investigated the temporal variation in fluorescence area of individual vesicles over a 60 s interval, employing the concept of proposed by Rosenfeld[32]. A threshold was selected based on shape compactness, and subsequently utilized to calculate the fuzzy geometric area[33]. In Fig. 1b, the images underwent processing using Image J software to derive the geometric area of the vesicles. As illustrated in Fig. 1c, it became apparent that with increasing concentrations of Ery, vesicles undergo significant

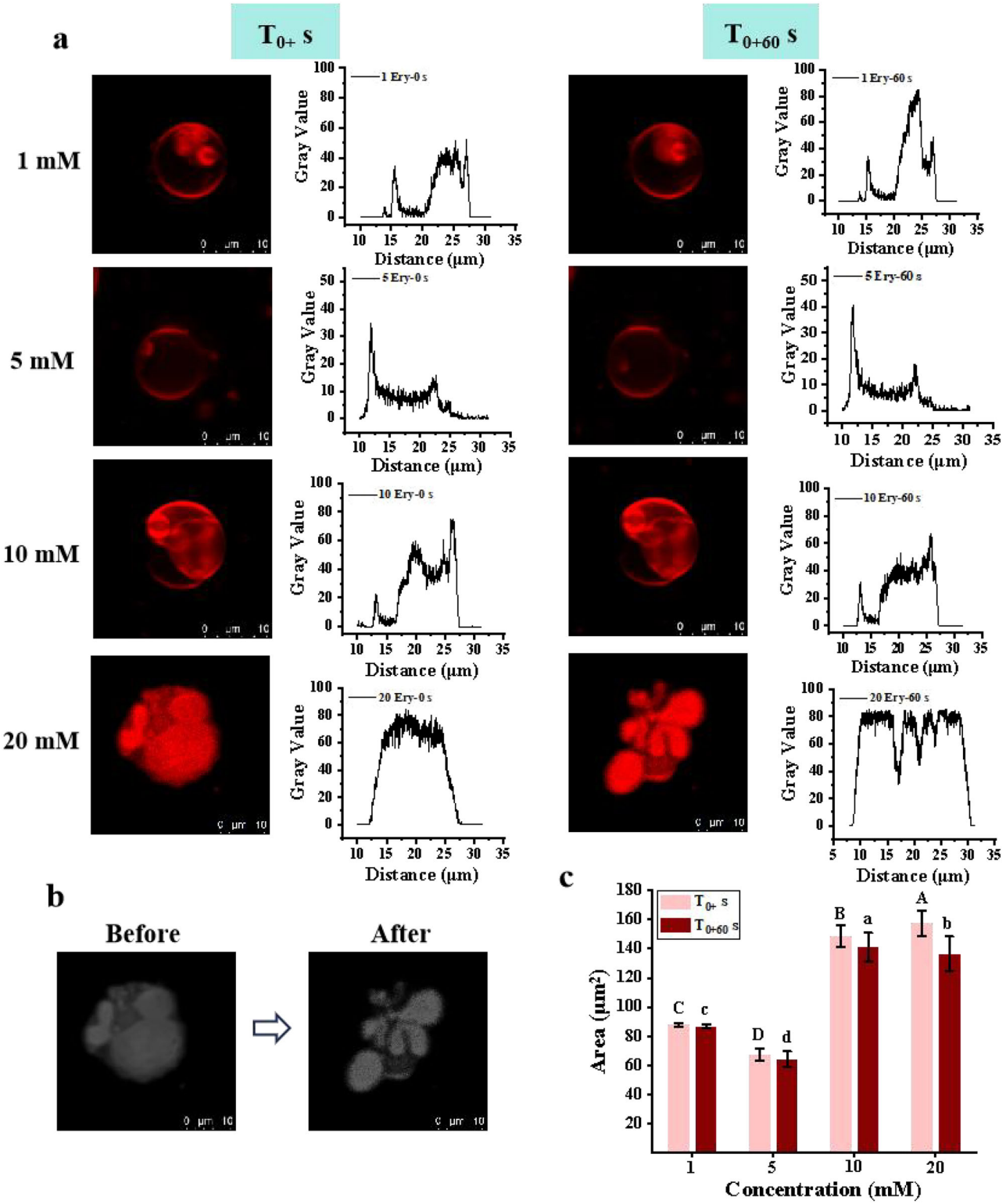

Fig. 1 | Representation of concentration-induced morphological changes in GUVs. a Morphology and location analysis of vesicles in the environment of Ery concentration increase. **b** Changes in GUV area over 60 s determined using the Rosenfeld algorithm. **c** GLV area in the presence of different concentrations of Ery at 0 s and 60 s, respectively. Different uppercase letters (A, B, C, D) or lowercase letters (a, b, c, d) within each sample group indicate significant differences between groups ($p < 0.05$). Uppercase letters are used to denote inter-group differences at T_{0+} s, while lowercase letters represent intra-group differences at T_{0+60} s.

morphological alterations, consistently supporting conclusions drawn from data analysis. Upon Ery's addition, the vesicle area diminished within 60 s. Elevated osmotic pressure in the solution prompted water within the membrane to diffuse outward, resulting in vesicle shrinkage. Vesicle area exhibited minimal variation when Ery concentrations were at or below 10 mM. Specifically, at 1 mM Ery concentration, the vesicle area decreased by 1.298 μm² over 60 s; at 5 mM, the decrease amounted to 3.016 μm²; and at 10 mM, the reduction was 7.593 μm². However, at 20 mM Ery concentration, the heightened osmotic pressure induced a looser arrangement of phospholipid bilayers, rendering them susceptible to rearrangement.

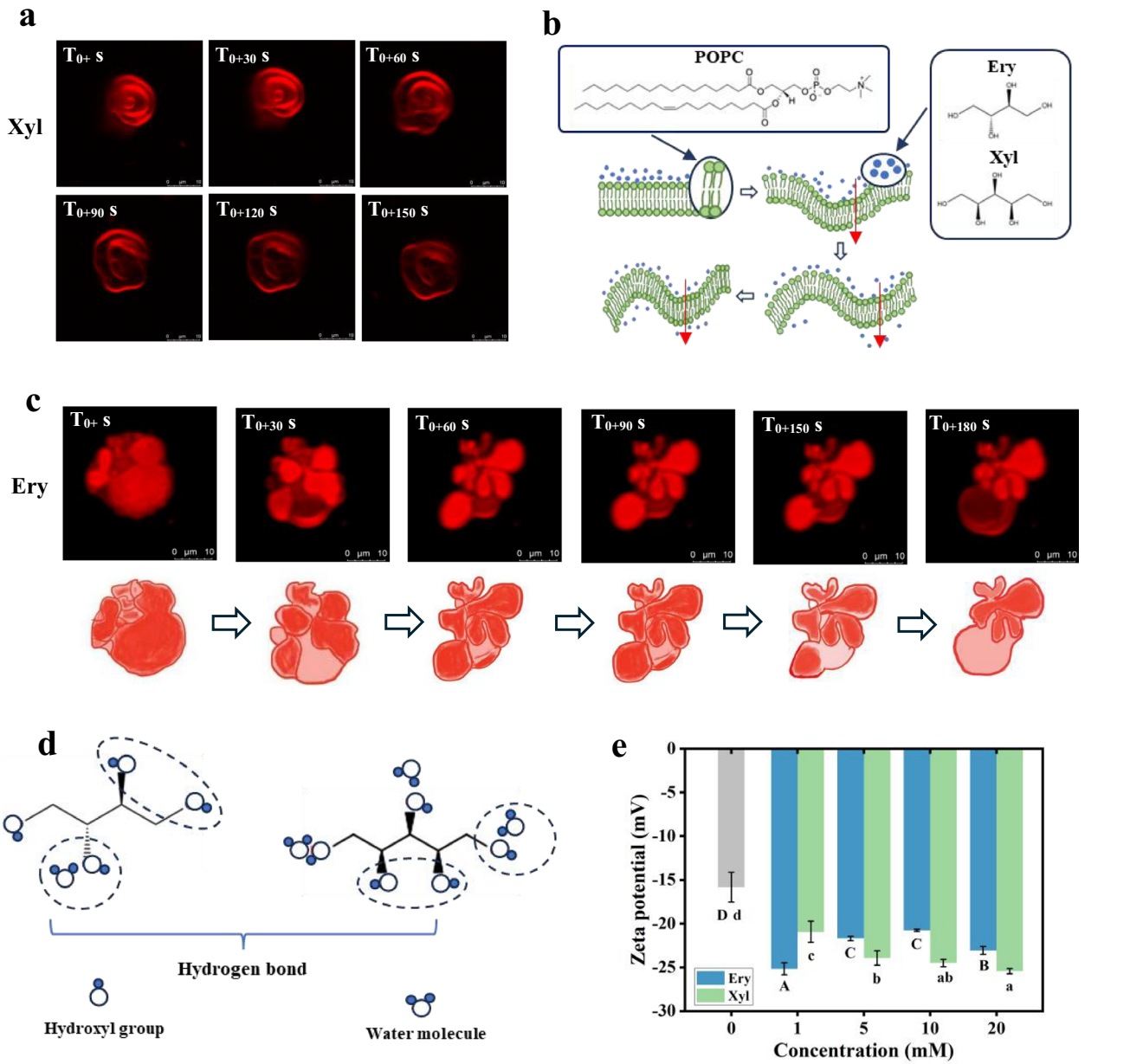

Fig. 2 | Perturbation of vesicles by hydrogen bonding in sugar alcohols. a 10 mM Xyl perturbed GUV folds. **b** Schematic representation of concentration-induced bending of phospholipid bilayer membranes by osmosis. **c** 20 mM Ery perturbed GUV deformation. **d** Schematic of hydrogen bond formation in Ery and Xyl molecules. **e** Zeta potential changes of vesicles under different concentrations of Ery and Xyl. The standard errors of the three parallel samples are represented by error bars. Different uppercase letters (A, B, C, D) or lowercase letters (a, b, c, d) in each sample group indicate significant differences between groups ($p < 0.05$). Intra-group differences of Ery are represented by uppercase letters, and intra-group differences of Xyl are represented by lowercase letters.

Both membrane permeability and morphology change when vesicle-mimicking cell membranes respond to changes in the environment. Previous studies have demonstrated that the exposure of vesicles to sucrose, glucose and other solutions induces fission, fusion, inward and outward germination due to osmotic stress[25,34]. Experimental results indicated that vesicles deform in response to osmotic stress induced by concentration increased. The osmotic pressure caused by 20 mM Ery results in irregular deformation of GUVs over a short period.

The varying molecular structures of sugar alcohols lead to deformations in GUVs

The aforementioned results suggested that osmotic pressure due to increasing concentration gradients results in morphological changes in vesicles, with a concentration of 20 mM Ery promoted vesicle deformation. At 10 mM Xyl environment, vesicles exhibited inward budding and were consistent with previous findings where high osmotic environments caused outward diffusion of water molecules, leading to vesicle membrane invagination and budding (As shown in Supplementary Fig. 4). Moreover, when the Xyl concentration increased to 20 mM, high osmotic stress-induced vesicle membrane semi-fusion, accompanied by membrane extension outward and a decrease in vesicle volume (Supplementary Fig. 5). Experimental results demonstrated that the Xyl environment at a concentration of 10 mM provided sufficient osmotic conditions to induce vesicle deformation. The permeation of sugar alcohol induces bending of the vesicle membrane (Fig. 2b). Specifically, the bending of the vesicle membrane is mainly due to the osmotic pressure difference created by the addition of external sugar alcohol solutions. Since sugar alcohol molecules cannot pass through the membrane, an increase in the concentration of sugar alcohols in

the external solution raises the external osmotic pressure, causing water molecules to flow out from inside the vesicle. This results in a reduction in vesicle volume while the membrane area remains relatively unchanged, thereby leading to bending and deformation of the membrane. Additionally, fluorescence images in Fig. 2a revealed that under a 10 mM Xyl environment, vesicles undergo inward contraction and wrinkling due to osmotic effects. Researches has shown that vesicles exhibited wrinkling phenomena under high osmotic stress. According to the van 't Hoff equation[35]:

$$\pi = kTc \quad (1)$$

where π represents osmotic pressure and c represents the concentration difference of solutes.

Different sugar alcohols at the same concentration theoretically produce the same osmotic pressure. However, the actual effects on vesicle morphology may vary due to factors such as specific molecular interactions (e.g., hydrogen bonding) or differences in membrane permeability. In this study, a 10 mM Ery environment did not induce significant morphological changes in vesicles, while a 20 mM Ery environment resulted in notable morphological alterations. As depicted in Fig. 2c, vesicles underwent continuous morphological transitions within 3 min. Additionally, we observed with astonishment that the accumulation of red fluorescence at 150 s unfolded into phospholipid layers by 180 s, suggesting that the accumulated red fluorescence may correspond to the stacking of phospholipid bilayers. The stacking and unfolding of phospholipid membranes might be associated with the high osmotic effects and hydrogen bonding provided by Ery, leading to changes in the characteristics of the phospholipid membrane.

Hydrogen bonding between sugar alcohols and phospholipid membranes has been extensively studied in the literature. For instance, Pereira et al. demonstrated that polyhydroxy compounds, such as sugar alcohols, can form hydrogen bonds with the polar head groups of phospholipids, leading to changes in membrane properties such as fluidity and permeability[16]. Similarly, Crowe et al. highlighted that sugars and sugar alcohols interact with membrane lipids through hydrogen bonding, which can stabilize or destabilize the membrane structure depending on the concentration and molecular structure of the sugar alcohol[15]. These studies support the notion that hydrogen bonding plays a significant role in the interaction between sugar alcohols and phospholipid membranes, contributing to the observed morphological changes in GUVs. Ery and Xyl are 4-carbon and 5-carbon polyhydroxy alcohols, respectively, with different arrangements and positions of hydroxyl groups. Additionally, the concentration disparity at which they perturb vesicle morphological changes was inconsistent, likely owing to differences in their molecular structures and hydroxyl group quantities. Research has shown that polyhydroxy alcohols had preferential affinity for the surface of phospholipid bilayers and were driven by hydrophobic interactions, leading to membrane swelling and disordered within the bilayer[16,36]. Therefore, the molecular structure and OH number of sugar alcohols might be facilitated the interaction with phospholipid molecules, altering the spontaneous curvature of the phospholipid membrane.

As shown in Fig. 2d, Ery and Xyl are polyhydroxy compounds, which the different hydroxyl groups within their molecules may form intramolecular hydrogen bonds. When dissolved in water, these sugar alcohols can form hydrogen bonds with water molecules. Due to the differing arrangements and positions of hydroxyl groups in the molecular structures of different sugar alcohols, they form distinct hydrogen bond networks in aqueous solutions. Formation of these hydrogen bond networks allowed sugar alcohol molecules to effectively interact with water molecules, thereby altering the distribution of water molecules in the solution and their own solubility and stability in water. As depicted in Fig. 2e, in different concentrations of Ery environment, the average zeta potential of phospholipid vesicles initially decreased and then increased, with the lowest potential observed when the Ery concentration was 1 mM. In Xyl environment, as the Xyl concentration increased, the average potential of phospholipid vesicles continuously decreased. Experimental results indicated that the addition of sugar alcohol solutions alters the charge distribution on the vesicle surface. Moreover, due to the structural and OH numbers were both different between Ery and Xyl, the effects of concentration on the change in surface zeta potential of vesicles varied.

Consequently, sugar alcohols tended to exhibit an affinity for the bilayer's surface region, surpassing that of water. The presence of polyhydroxy co-solute molecules replaced some water molecules at hydrogen-bonding sites provided by the membrane, particularly at ester group levels[16]. Therefore, the part of reason about deformation of GUVs could be attributed to differences in the arrangement position and number of hydroxyl groups present in sugar alcohols. Hydrogen bonds can be formed between the hydroxyl group of sugar alcohol molecule and phospholipid group or fatty acid group, and this interaction can increase the binding ability between sugar alcohol molecule and phospholipid molecule. In addition, van der Waals forces interact between the hydrophobic part of the sugar alcohol molecule and the hydrophobic tail group of the phospholipid molecule, further enhancing the attraction between them. These interactions can lead to the formation of adsorption layers on the surface of phospholipid molecules, thus changing the arrangement of phospholipid molecules and the properties of the membrane.

The cytotoxic effects influenced by sugar alcohols and a notable reduction in ROS levels

In order to further investigate the molecular-level mechanisms by which sugar alcohols facilitate membrane penetration and adsorption, we assessed cell viability, ROS levels, membrane adsorption and membrane potential on HEK-293 cells. Cell viability plays a crucial role in a variety of different biological systems, and normal cell cycles, morphological changes, and chemical induction cause cell death[37]. As shown in Fig. 3a, the Con group represented a sugar-alcohol-free culture medium. In Ery and Xyl environments, although cell viability gradually decreased with increasing sugar alcohol concentration, HEK-293 cells maintained over 80% viability at exposure levels of 25 mM compared to the control group. Therefore, concentrations ranging from 0 to 20 mM were selected for subsequent cellular experiments.

Subsequently, we measured the fluorescence intensity expressed by the DCFH-DA probe to assess the intracellular levels of ROS and performed quantitative analysis of the fluorescence. The data presented in Fig. 3b showed that the ratio of fluorescence values within HEK-293 cells exposed to sugar alcohol environments for 24 h compared to the control group. With increasing concentrations of Ery and Xyl, intracellular ROS levels exhibited a significant decrease ($P < 0.05$), with Ery exerting a pronounced reduction in ROS levels followed by Xyl. Cell viability is closely related to the generation of intracellular ROS; thus, it plays a significant role in ROS production. However, even with cell viability exceeding 80%, higher concentrations of Ery and Xyl led to ROS levels decreasing below 0.8. The experimental results suggested that the reduction in intracellular ROS levels may be attributed to the interaction of Ery and Xyl with the cell membrane, leading to changes in membrane permeability and subsequent cellular responses. Previous studies have shown that osmotic stress induced by solutes can trigger cellular stress responses, including changes in ion exchange, water flux, and cell volume, which may influence ROS generation and scavenging pathways[38,39]. Additionally, the hydroxyl groups in Ery and Xyl may interact with membrane lipids, potentially affecting the membrane's physical properties and its response to osmotic stress[40]. These combined effects could explain the observed reduction in ROS levels, without necessarily implying direct antioxidant activity.

Sugar alcohols have a significant impact on the membrane potential of HEK-293 cells

Cell membrane potential was a fundamental property of biological cells, and its variations represented a large number of essential activities in biology[41]. Common strategies for recording changes in membrane potential that occurred during chemical reactions induced the use of organic dyes or gene-encoded voltage indicators with voltage-dependent fluorescence[42–44]. The

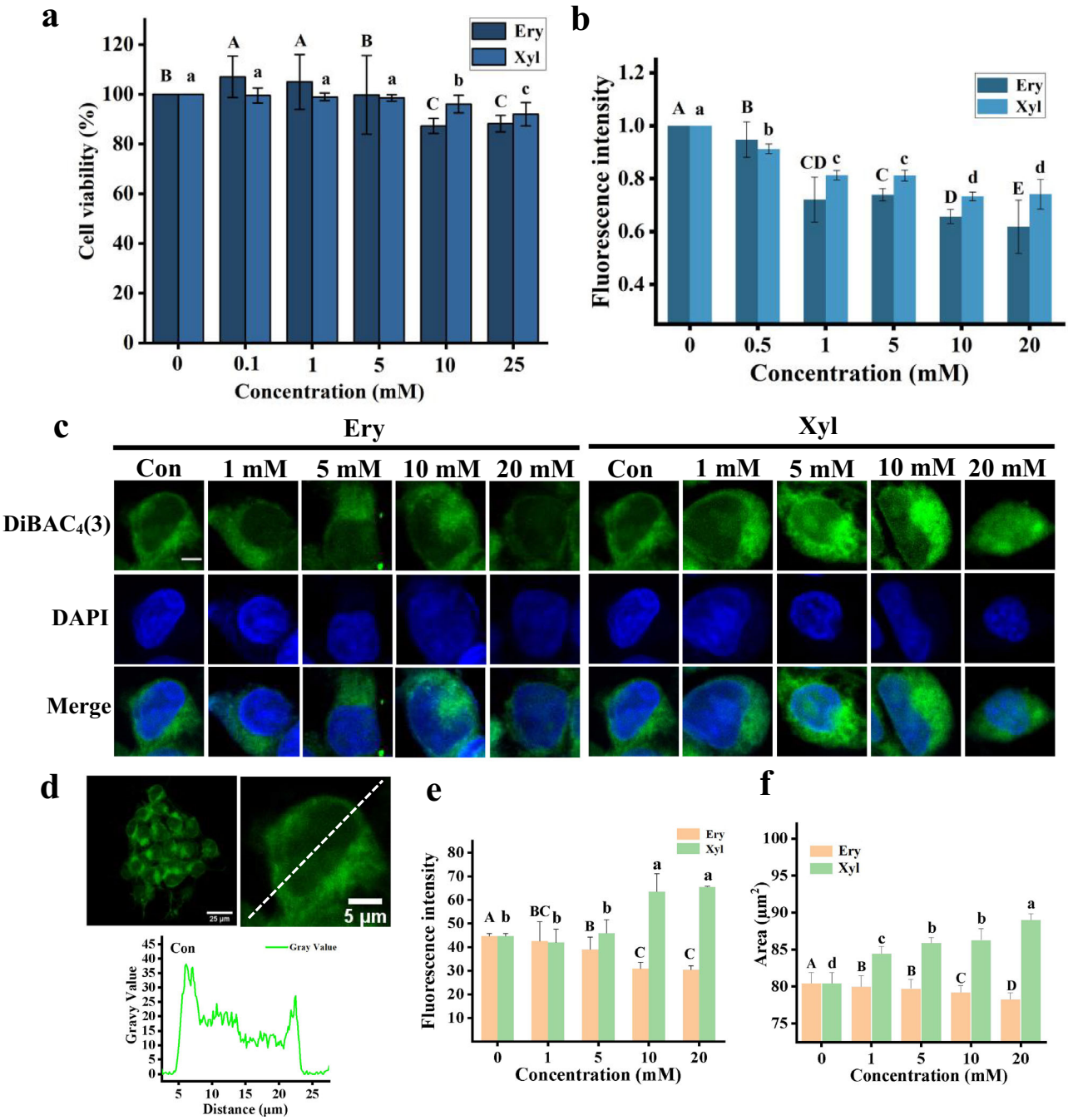

Fig. 3 | Physiological characterization of HEK-293 cells in different concentrations of Ery and Xyl environments. a Cell viability under different concentrations of Ery and Xyl. **b** ROS production in cells under different concentrations of Ery and Xyl ($P < 0.05$). **c** CLSM diagram of cell membrane potential under different concentrations of Ery and Xyl, DiBAC4(3) indicated membrane permeability, DAPI labeled nuclei, scale bar is 5 μm. **d** Analysis of fluorescence distribution within the cell membrane. **e** Fluorescence quantification analysis of green fluorescence in CLSM plot S6. **f** Analysis of changes in membrane potential of cells perturbed by different concentrations of Ery and Xyl environments within 2 h period. The standard errors of the three parallel samples are represented by error bars. Different uppercase letters (A, B, C, D) or lowercase letters (a, b, c, d) in each sample group indicate significant differences between groups ($p < 0.05$). Intra-group differences of Ery are represented by uppercase letters, and intra-group differences of Xyl are represented by lowercase letters.

purpose of measuring cell membrane potentials in solution is to investigate the role of the solution medium in facilitating membrane contact and evaluate its functional implications. The DiBAC4(3) probe was a potential sensitive probe of the cell membrane that could bind to cellular proteins and emit green fluorescence. In the present study, a DiBAC4(3) fluorescent probe was used to label the HEK-293 cell membrane to indicate the influence of the sugar alcohol environments on cell membrane potential.

Supplementary Fig. 6 presents CLSM fluorescence micrographs of cells under different concentrations of Ery and Xyl environments. As shown in the Fig. 3c, by enlarging the image, the fluorescence in a single cell was analyzed. At the presence of Ery, as the concentration increased, HEK-293 cells contracted, and the intracellular green fluorescence dimmed. Conversely, in the presence of Xyl, as the concentration increased, cells contracted, and the intracellular green fluorescence intensified. The intensity of fluorescence reflects the degree of cell membrane polarization, thus indicating membrane permeability. As shown in Fig. 3d, the DiBAC4(3) probe was evenly distributed within the cell membrane, and grayscale values were obtained through linear proportion to construct a more precise quantitative

assessment, exploring the impact of different concentrations of Ery and Xyl on cell membrane permeability. Similarly, fluorescence quantification values were obtained as shown in Fig. 3e. The results indicated that with increasing Ery concentration, cell membrane potential decreased, became hyperpolarized, with higher Ery concentrations associated with lower membrane permeability. Conversely, Xyl yielded opposite results. With increasing Xyl concentration, cell membrane potential increased, led to depolarization and increased membrane permeability. To further elucidate the effects of the two sugar alcohols on HEK-293 cell membrane permeability, changes in fluorescence within the cell membrane were tracked and recorded over a period of 2 h, followed by analysis of the synthesized data curves (Fig. 3f). As mentioned above, these findings were consistent with the aforementioned results: increasing Ery concentration hyperpolarizes the cell membrane, decreasing membrane permeability, while increasing Xyl concentration depolarizes the cell membrane, increasing membrane permeability.

These experimental results demonstrated that as the concentration of sugar alcohols increases, Ery inhibits the permeability of HEK-293 cell membranes, whereas Xyl increases membrane permeability. Moreover, under the same concentration-induced osmotic conditions, differences existed in the alterations of membrane permeability of HEK-293 cells induced by Ery and Xyl, which were likely associated with the molecular structure of the sugar alcohols and their hydrogen bonding interactions. Therefore, the polyol structures were capable of binding with phospholipid molecules, thereby altering the properties of the phospholipid membrane.

High concentrations of sugar alcohol greatly enhance the adsorption of vesicles onto cell membranes via an osmotic effect

To investigate whether the physical state of cell membranes and the high osmotic properties of different sugar alcohols affect the adsorption of vesicles around the cell membrane, we measured the fluorescence intensity emitted by labeled vesicles using a fluorescence probe. Prior to conducting experiments perturbing cell membrane adsorption with sugar alcohols, cell viability was assessed. Cell viability assays conducted under different vesicle concentration conditions revealed that cell viability decreased to less than 80% when the vesicle concentration exceeded 2 mg/mL. Consequently, a vesicle concentration of 1 mg/mL was chosen for subsequent experiments. Additionally, when cells were co-cultured with vesicles in a 20 mM sugar alcohol environment for 24 h, cell viability remained above 90%, indicating their suitability for further experimentation (Fig. 4a). Following 4 h of co-culture of HEK-293 cells with vesicles in various sugar alcohol environments, samples were removed and washed with PBS to remove unabsorbed vesicles from the cell membrane. Subsequently, DAPI was used to label cell nuclei for cell positioning, and vesicle distribution was observed under a microscope.

CLSM fluorescence images demonstrated an increasing number of vesicles adhering to the cells in microenvironments with different concentrations of sugar alcohols. Image analysis using Image J software enabled fluorescence quantification, as depicted in Fig. 4b, c, indicating that vesicle adsorption on the cell membrane was significantly higher in environments containing 10 mM and 20 mM Ery and Xyl compared to the control environment of simple culture medium, due to the osmotic effect. CLSM images clearly indicated that the osmotic action of sugar alcohols led to increased vesicle adsorption on the cell membrane. Furthermore, quantitative analysis of fluorescence revealed that the osmotic action of sugar alcohols significantly enhanced vesicle adsorption on the cell membrane. Moreover, as shown in Fig. 4d, it was observed that vesicle adsorption was significantly higher in the 5 mM Xyl environment compared to the control group, whereas there was no significant difference in the Ery environment at the same concentration. Additionally, in 10 mM and 20 mM sugar alcohol environments, vesicle adsorption was higher in the Xyl environment than in the Ery environment at the same concentration, indicating that Xyl provided a higher osmotic effect than Ery, thereby promoting vesicle adsorption on the cell membrane. To further illustrate that vesicle adsorption on the cell membrane was higher in the Xyl environment than in the Ery environment at the same concentration, we performed 3D scans of vesicle adsorption on cells in environments containing 20 mM Ery and Xyl (Fig. 4e).

Although sugar alcohols are small molecules, they cannot freely diffuse through the phospholipid membrane, thus providing a highly permeable environment that promotes vesicle adsorption on cells. Considering that the diffusion of sugar alcohols through the cell membrane may occur via simple diffusion and is molecule-dependent, with Xyl having a larger molecular weight than Ery, the lipid portion of the cell membrane may be more permeable to Ery molecules. Our conclusion was that in high sugar alcohol concentrations, in addition to the osmotic effect, membrane fluidity and packing density are altered by the properties of Ery and Xyl, resulting in changes in cell membrane permeability.

Experimental section

Materials

Erythritol (98%, purity), xylitol (99%, purity) were purchased from Macklin Biochemical Technology (Shanghai, China). 1-Palmitoyl-2-oleoyl-sn-glycerol-3-phosphocholine (POPC, ≥98%), and the fluorescent dyes 1,1'-dioctadecyl-3,3,3',3'-tetramethylindocarbocyanine perchlorate (DiI), 4',6-Diamidine-2'-phenylindole dihydrochloride (DAPI, ≥98%), Bis-(1,3-dibutylbarbituric acid) trimethine oxonol (DiBAC4(3), ≥95%) and 2',7'-Dichlorodihydrofluorescein diacetate (DCFH-DA, ≥95%), were purchased from Sigma-Aldrich (Shanghai, China). 3-(4,5dimethylthiazol-2-yl)-2,5-diphenyltetrazolium bromide (MTT) was purchased from Aladdin Chemistry Co., Ltd (Shanghai, China). Milli-pore water (18 MΩ) was attained from Millipore Gradient Milli-Q. All the reagents are analytical grade unless otherwise stated.

Preparation of giant unilamellar vesicles (GUVs)

Based on the previous experiments[45], GUVs were prepared by a film hydration method. In brief, 10 mg/mL POPC phospholipids and fluorescent dye DiI (whose quality is 1/1000 of that of POPC) were dissolved in chloroform together in a round-bottom flask. The chloroform removed under a flow of nitrogen gas and then a lipid film was deposited on the surface of a flask. The lipid film was subsequently pre-hydrated with Milli-Q water and the swelling process for two hours or more, 2 mg/mL liposome vesicle solution was generated.

Preparation and addition of sugar alcohol solution

Before the start of the experiment, 500 mM solutions of Ery and Xyl were prepared, and sugar alcohol solutions with concentration gradients of 2 mM, 10 mM, 20 mM, and 40 mM were designed. After preparing the GUVs solution, it was transferred to the microscope observation chamber to ensure the GUVs were stably suspended. Prior to observation, the pre-prepared sugar alcohol solution was quickly added to the GUVs solution. The sugar alcohol solution and vesicle solution were mixed at a volume ratio of 1:1 (VV/VS = 1:1), ensuring the final sugar alcohol concentration reached the experimental target. The sugar alcohol solution was added using a micropipette, slowly injected along the wall of the observation chamber to avoid mechanical disturbance to the GUVs. After the addition, the solution was allowed to stand for 120 s to reach dynamic homeostasis equilibrium before being observed using confocal microscopy. Images were recorded at a frequency of every 3 s, and the moment of observation was defined as "T_{0+} s" after the sugar alcohol was added and left for 120 s.

Observation of morphological changes of GUVs

The fluorescent microscopic observations of GUVs were performed using a laser confocal microscope (CLSM, Leica TCS-SP8 SR, Germany). The probe DiI generated fluorescence after binding to POPC molecules, and the GUVs shape could be observed at the Ex/Em = 463/536 nm. When various types of sugar alcohols were added to the vesicle solution, GUVs were observed the formation of protrusions and self-splitting behavior owing to the osmotic stress. The images were recorded with the HC PL APO CS2 40/1.30 OIL objective and were recorded once every 3 s.

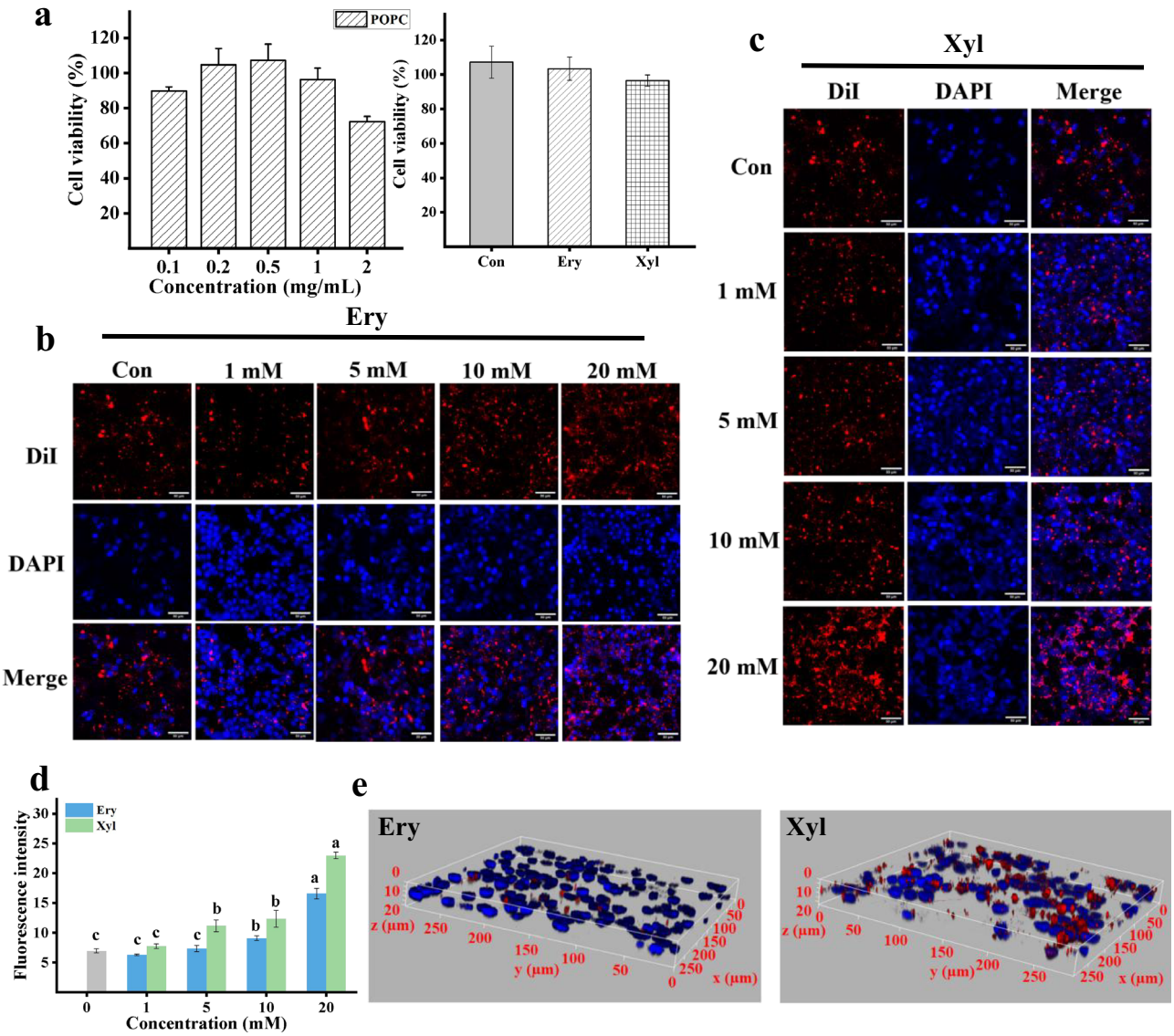

Fig. 4 | Effect of different concentrations of Ery and Xyl treated vesicles on their membrane adsorption and cell viability in HEK-293 cells. a Impact of different concentrations of vesicles, Ery and Xyl environment treated vesicles on cell viability. CLSM plots of vesicle adsorption on cell membranes at different concentrations of sugar alcohol environments, (**b**) Ery and (**c**) Xyl, DiI labeled vesicles, DAPI-labeled nuclei, scale bar of 50 μm. **d** Mean amount of fluorescence of vesicles adsorbed on the cells ($P < 0.05$). **e** 3D plot of vesicle adsorption on cells in 20 mM Ery, Xyl respectively. The standard errors of the three parallel samples are represented by error bars.

Measurement of the zeta potential of GUVs

The mean zeta potential of vesicles was measured by Malvern Zetasizer Nano ZS90 (Malvern Instruments, UK). Vesicle solution was mixed with the sugar alcohol solution to achieve the concentration of the vesicle solution was 1 mg/mL. All measurements were made three times at 25 °C following 20 min equilibration interval.

Cell experiments

Cell culture and cell viability assay. HEK-293 cells were cultured in an incubator (Binder, Tuttlingen, Germany) at 37 °C, 95% air humidity and 5% CO_2. When the cell density reached 80%, the cells were treated with 0.25% trypsin and cell passaging was performed. HEK-293 cells were cultured with the medium, which consisted of 10% FBS and 90% DMEM medium (containing 1% double antibody). Cells were respectively seeded in 96-well plates at a density of 1.0×10^5 cells/mL and 6-well plates at a density of 1.0×10^4 cells/mL and incubated for 24 h to experiment.

The viability of HEK-293 cell using the MTT method to measure[46]. Different concentrations of sugar alcohols were added to the wells to incubate 24 h. 20 μL 0.5 mg/mL MTT was added to each well and incubated for 4 h. Using multifunction microplate reader (Flexstation3, USA), the absorbance of formed formazan was measured at 570 nm.

Measurement of intracellular ROS. The experimental procedures were as previously described by Liu et al. with slight modifications[47]. The cells were pretreated with 10 mM different sugar alcohols were respectively added in the wells and incubated for 24 h; then, DCFH-DA dissolved in DMEM medium (at a ratio of 1:1000) was added to each well and incubated for 20 min. After that, the cells were washed three times with PBS to remove extracellular DCFH-DA, and the fluorescence intensity was detected under a multifunction microplate reader with Ex/Em = 488/525 nm. The fluorescence readings represent the average fluorescence intensity of the entire cell population within each well. Each experimental condition was performed in triplicate wells across three independent experiments ($n = 3$) to ensure reliability and reproducibility of the results.

Cell membrane potential. The measurements of the membrane potential were carried out using the earlier methods[48]. 100 μL of 5 μM DiBAC4(3) was added in wells and incubated for 15 min in the incubator.

Then, 100 μL of samples were added to wells and tested samples were detected by a multifunction microplate reader (Flexstation3, USA) every 10 min for 120 min at 37 °C, Ex/Em = 493/516 nm was for set. The fluorescent micrographs were taken immediately after the fluorometric experiment (DiBAC4(3): Ex/Em = 493/516 nm; DAPI: Ex/Em = 340/450 nm). All the samples were captured with four images. Fluorescence intensity was quantified from the captured images to assess membrane potential changes in the cells. Each experimental condition was performed in triplicate across three independent experiments ($n = 3$) to ensure reliability and reproducibility of the results.

Cellular membrane adsorption. According to Wang et al. HEK-293 cells were incubated for 24 h and later observed with a light microscope[49]. 1 mM vesicles with various sugar alcohols were then added to the cells for 4 h. Then, the cells washed with PBS and fixed with 4% paraformaldehyde for 10 min, nuclei were labeled with DAPI for 15 min and then washed twice with PBS. Imaging was acquired using the CLSM (DiI: Ex/Em = 463/536 nm; DAPI: Ex/Em = 340/450 nm). All the samples were captured with four images.

Image and data analysis

Results were expressed as mean ± standard deviation. Each experiment was performed at least three times. Differences between means were compared by Duncan's test, and the significance level was set at $P < 0.05$, plots were made using Origin 2018 software. Fluorescent micrographs processed by Image J.

Data availability

All the raw data presented have been provided as 'source data' for the respective figures. Owing to the large size of high-resolution microscopy images, the raw microscopy images are available from the corresponding author upon reasonable request.

Received: 2 December 2024; Accepted: 20 March 2025;
Published online: 30 March 2025

References

1. Zhou, M. et al. Mortality, morbidity, and risk factors in China and its provinces, 1990–2017: a systematic analysis for the Global Burden of Disease Study 2017. *Lancet* **394**, 1145–1158 (2019).
2. Kawano, Y. et al. Microbiota imbalance induced by dietary sugar disrupts immune-mediated protection from metabolic syndrome. *Cell* **185**, 3501–3519.e20 (2022).
3. Zuo, Q.-L. et al. Influences of xylitol consumption at different dosages on intestinal tissues and gut microbiota in rats. *J. Agric. Food Chem.* **69**, 12002–12011 (2021).
4. Castro-Muñoz, R. et al. Natural sweeteners: sources, extraction and current uses in foods and food industries. *Food Chem.* **370**, 130991 (2022).
5. Kikuko, A. et al. Effects of xylitol on metabolic parameters and visceral fat accumulation. *J. Clin. Biochem. Nutr.* **49**, 1–7 (2011).
6. Kishore, P. et al. Xylitol prevents NEFA-induced insulin resistance in rats. *Diabetologia* **55**, 1808–1812 (2012).
7. Uebanso, T. et al. Effects of consuming xylitol on gut microbiota and lipid metabolism in mice. *Nutrients* **9**, 756 (2017).
8. Godswill, A. C., Sugar alcohols: chemistry, production, health concerns and nutritional importance of mannitol, sorbitol, xylitol, and erythritol. *Int. J. Adv. Acad. Res*. **3**, 31–66 (2017).
9. Tomonobu, N. et al. Xylitol acts as an anticancer monosaccharide to induce selective cancer death via regulation of the glutathione level. *Chem. Biol. Interact.* **324**, 109085 (2020).
10. Kim, S., Park, M.H., Song, Y.R., Na, H.S. & Chung, J. Aggregatibacter actinomycetemcomitans-induced AIM2 inflammasome activation is suppressed by xylitol in differentiated THP-1 macrophages. *J. Periodontol.* **87**, e116–e126 (2016).
11. Lu, X., Li, C., Wang, Y.-K., Jiang, K. & Gai, X.-D. Sorbitol induces apoptosis of human colorectal cancer cells via p38 MAPK signal transduction. *Oncol. Lett.* **7**, 1992–1996 (2014).
12. Nagsuwanchart, P., Nakornchai, S., Thaweboon, S. & Surarit, R. Mogroside, palatinose, erythritol, and xylitol differentially affect dental plaque pH in caries-active and caries-free children: an in vitro study. *Pediatr. Dent. J.* **31**, 242–247 (2021).
13. Hulbah, M., Croxen, M.A. & Tyrrell, G.J. Phenotypic changes in group B streptococci grown in the presence of the polyols, erythritol, sorbitol and mannitol. *BMC Microbiol.* **21**, 145 (2021).
14. Yu, Z. & Guo, J. Non-caloric artificial sweeteners exhibit antimicrobial activity against bacteria and promote bacterial evolution of antibiotic tolerance. *J. Hazard. Mater.* **433**, 128840 (2022).
15. Crowe, J.H. et al. Interactions of sugars with membranes. *Biochim. Biophys. Acta Rev. Biomembr.* **947**, 367–384 (1988).
16. Pereira, C.S. & Hünenberger, P.H. The influence of polyhydroxylated compounds on a hydrated phospholipid bilayer: a molecular dynamics study. *Mol. Simul.* **34**, 403–420 (2008).
17. Yuan, W., Piao, J. & Dong, Y. Advancements in the preparation methods of artificial cell membranes with lipids. *Mater. Chem. Front.* **5**, 5233–5246 (2021).
18. Tian, J.-Q. et al. Interfacial energy-mediated bulk transport across artificial cell membranes. *Nat. Chem. Eng.* **1**, 450–461 (2024).
19. Mezzenga, R. et al. Nature-Inspired design and application of lipidic lyotropic liquid crystals. *Adv. Mater.* **31**, 1900818 (2019).
20. Chandrawati, R. & Caruso, F. Biomimetic liposome-and polymersome-based multicompartmentalized assemblies. *Langmuir* **28**, 13798–13807 (2012).
21. Kayingo, G., Kilian, S.G. & Prior, B.A. Conservation and release of osmolytes by yeasts during hypo-osmotic stress. *Arch. Microbiol.* **177**, 29–35 (2001).
22. Chabanon, M., Ho, J.C., Liedberg, B., Parikh, A.N. & Rangamani, P. Pulsatile lipid vesicles under osmotic stress. *Biophys. J.* **112**, 1682–1691 (2017).
23. Blount, P., Schroeder, M.J. & Kung, C. Mutations in a bacterial mechanosensitive channel change the cellular response to osmotic stress. *J. Biol. Chem.* **272**, 32150–32157 (1997).
24. Hasan, S. et al. Influence of sugar concentration on the vesicle compactness, deformation and membrane poration induced by anionic nanoparticles. *Plos one* **17**, e0275478 (2022).
25. Zong, W., Li, Q., Zhang, X. & Han, X. Deformation of giant unilamellar vesicles under osmotic stress. *Colloids Surf. B Biointerfaces* **172**, 459–463 (2018).
26. Chen, L., Xue, S., Dai, B., Wang, Y. & Zhao, H. Sucrose osmotic self-oscillation drives membrane permeability. *J. Agric. Food Chem.* **71**, 7557–7565 (2023).
27. Schelegueda, L.I., Zalazar, A.L., Herbas, E.T., Gliemmo, M.F. & Campos, C.A. Effect of gellan gum, xylitol and natamycin on Zygosaccharomyces bailii growth and rheological characteristics in low sugar content model systems. *Int. J. Biol. Macromol.* **164**, 1657–1664 (2020).
28. Rumiana Dimova, C. M. M., *The Giant Vesicle Book*. (CRC Press, Taylor & Francis Group: 2020).
29. Lasic, D.D. The mechanism of vesicle formation. *Biochem. J.* **256**, 1 (1988).
30. Takiue, T. Heterogeneity and deformation behavior of lipid vesicles. *Curr. Opin. Colloid Interface Sci.* **62**, 101646 (2022).
31. Bhatia, T., Robinson, T. & Dimova, R. Membrane permeability to water measured by microfluidic trapping of giant vesicles. *Soft Matter* **16**, 7359–7369 (2020).
32. Rosenfeld, A. The fuzzy geometry of image subsets. In *Readings in Fuzzy Sets for Intelligent Systems*, 633–639 (Elsevier, 1993).
33. Sezgin, M. & Sankur, B.I. Survey over image thresholding techniques and quantitative performance evaluation. *J. Electron. imaging* **13**, 146–168 (2004).

34. Liu, X., Stenhammar, J., Wennerstrom, H. & Sparr, E. Vesicles balance osmotic stress with bending energy that can be released to form daughter vesicles. *J. Phys. Chem. Lett.* **13**, 498–507 (2022).
35. Koslov, M. & Markin, V. A theory of osmotic lysis of lipid vesicles. *J. Theor. Biol.* **109**, 17–39 (1984).
36. Tammela, P. et al. Permeability characteristics and membrane affinity of flavonoids and alkyl gallates in Caco-2 cells and in phospholipid vesicles. *Arch. Biochem. Biophys.* **425**, 193–199 (2004).
37. Grasmann, G., Smolle, E., Olschewski, H. & Leithner, K. Gluconeogenesis in cancer cells–repurposing of a starvation-induced metabolic pathway?. *Biochim. Biophys. Acta Rev. Cancer* **1872**, 24–36 (2019).
38. Mager W. H., de Boer A. H., Siderius M. H., Voss H. P.; Cellular responses to oxidative and osmotic stress. (Cell stress & chaperones, 2000).
39. Burg, M.B., Ferraris, J.D. & Dmitrieva, N.I. Cellular response to hyperosmotic stresses. *Physiol. Rev.* **87**, 1441–1474 (2007).
40. Budziak, I. et al. Effect of polyols on the DMPC lipid monolayers and bilayers. *Biochim. Biophys. Acta Biomembr.* **1860**, 2166–2174 (2018).
41. Abdul Kadir, L., Stacey, M. & Barrett-Jolley, R. Emerging roles of the membrane potential: action beyond the action potential. *Front. Physiol.* **9**, 1661 (2018).
42. Nikolaev, D.M. et al. Fluorescence imaging of cell membrane potential: From relative changes to absolute values. *Int. J. Mol. Sci.* **24**, 2435 (2023).
43. Oh, S. et al. Label-free imaging of membrane potential using membrane electromotility. *Biophys. J.* **103**, 11–18 (2012).
44. Chen, G. et al. Glutathione-capped quantum dots for plasma membrane labeling and membrane potential imaging. *Nano Res.* **12**, 1321–1326 (2019).
45. Reeves, J.P. & Dowben, R.M. Formation and properties of thin-walled phospholipid vesicles. *J. Cell. Physiol.* **73**, 49–60 (1969).
46. Wang, X. et al. Analysis of the in vivo and in vitro effects of photodynamic therapy on breast cancer by using a sensitizer, sinoporphyrin sodium: erratum. *Theranostics* **11**, 7126 (2021).
47. Liu, J. et al. Anti-oxidative and anti-apoptosis effects of egg white peptide, Trp-Asn-Trp-Ala-Asp, against H_2O_2-induced oxidative stress in human embryonic kidney 293 cells. *Food Funct.* **5**, 3179–3188 (2014).
48. Wang, H. et al. Isolation of colloidal particles from porcine bone soup and their interaction with murine peritoneal macrophage. *J. Funct. Foods* **54**, 403–411 (2019).
49. Wang, X. et al. Enhanced drug delivery using sonoactivatable liposomes with membrane-embedded porphyrins. *J. Control. Release* **286**, 358–368 (2018).

Acknowledgements

This work was supported by funding from the National Natural Science Foundation of China (NSFC, 32072218, 31741101), the China Scholarship Council (CSC 202108330160), the Zhejiang Science Technology Project (No. 2018C02054).

Author contributions

Lichun Chen: Conceptualization, data curation, formal analysis, investigation, funding acquisition, methodology, visualization. Feng Yao: Resources, writing-review & editing. Songwen Xue: Conceptualization, investigation, methodology, writing-original draft, project administration, supervision. Kuang Yao: Writing-review & editing. Yun Huang: Writing-review & editing. Huimin Zhao: Writing-review & editing. Qiong Shao: Conceptualization, funding acquisition, project administration, resources, supervision, writing-review and editing. All authors read and approved the final manuscript.

Competing interests

The authors declare no competing interests.

Additional information

Supplementary information The online version contains supplementary material available at https://doi.org/10.1038/s41538-025-00410-1.

Correspondence and requests for materials should be addressed to Qiong Shao.